Molecular hydrogen physisorption on boron-nitride nanotubes probed by second harmonic generation

R. V. Salazar-Aparicio, R. A. Vázquez-Nava,* N. Arzate, and B. S. Mendoza
Centro de Investigaciones en Optica A. C., León, Guanajuato, México
(Received 30 May 2014; revised manuscript received 3 September 2014; published 2 October 2014)

We present *ab initio* calculations to investigate second harmonic generation (SHG) response of single wall zigzag pristine boron-nitride nanotubes (BNNTs) and BNNTs modified by the molecular hydrogen adsorption. Calculations have been performed using density functional theory (DFT) within the local-density approximation (LDA) together with the GW Green function method to determine the band gap. A length gauge approach has been used to calculate the nonlinear optical response with the scissors correction to obtain the nonlinear susceptibility $\chi^{zzz}(-2\omega;\omega,\omega)$ of the zigzag BNNTs. We have found that, contrary to reports in the literature, the (5,0) and (9,0) BNNTs have a nonvanishing SHG response. We have also found that SHG intensity decreases with the increase of the molecular hydrogen coverage.

DOI: 10.1103/PhysRevB.90.155403 PACS number(s): 78.67.Ch, 73.20.−r, 88.30.R−

I. INTRODUCTION

During the past decade, nanotube (NT) surfaces have been the subject of recent activity and investigation since they may be used technologically in gas sensors [1–4], hydrogen storage devices [5–10], or to remove toxic gases [11,12]. To date, the adsorption of several molecules such as fluorine, methanol, H_2, O_2, CO_2, C_2H_2, and H_2O [13–18] on NT surfaces has been investigated. In particular, hydrogen adsorption on boron-nitride nanotubes (BNNTs) has drawn intense research interest because they have been considered as potential H_2-storage media. A number of theoretical studies of H atoms [19,20] or H_2 molecules [5,7–10] adsorption on BNNTs have been published in the literature. The H_2 molecules adsorption on BNNT is essentially physical in nature and depends on electrostatic and weak Van der Waals interactions.

Our interest in this paper is to show that second harmonic generation (SHG) is a powerful spectroscopic tool to study optical properties of NT surfaces since it has the advantage of being surface sensitive. For centrosymmetric materials inversion symmetry forbids, within the dipole approximation, SHG from the bulk, but it is allowed at the surface, where the inversion symmetry is broken. Therefore, SHG should necessarily come from a localized surface region. SHG allows us to study the structural atomic arrangement and phase transitions of clean and adsorbate covered surfaces [21], and since it is an optical probe, it can be used out of UHV conditions and is noninvasive and nondestructive [22]. On the experimental side, the new tunable high intensity laser systems have made SHG spectroscopy readily accessible and applicable to a wide range of systems.

Recently, Guo and Lin [23] have systematically studied *ab initio* second-order nonlinear optical properties of pristine BNNTs within density-functional theory (DFT) based on the independent particle approximation (IPA). They found that zigzag BNNT's exhibit large SHG behavior compared to that of bulk BN. Also, Margulis *et al.* [24] have investigated theoretically the $\chi^{zzz}(-2\omega;\omega,\omega)$ component of zigzag BNNTs within the simple model based on a two-band tight-binding approximation. They found that the SHG spectrum is dominated by a highly peaked 2ω resonance at half the band gap energy of the pristine BNNT.

Here, we present *ab initio* calculations to investigate SHG response of single wall zigzag pristine BNNTs and BNNTs modified by the molecular hydrogen adsorption. Our calculations are performed at the level of the IPA by considering GW energy corrections [25] through the application of a scissors operator. We have found that SHG spectrum of the (6,0) BNNT exhibits similar features to those reported by Guo and Lin, but in the case of the (5,0) and (9,0) BNNTs we found a nonvanishing SHG reponse, contrary to that found by Guo and Lin. Also all the features in the spectra are produced by two-photon transitions close to the Γ point at the center of the Brillouin zone in a similar way to that reported by Margulis *et al.*

The layout of the paper is as follows. In Sec. II, we present our theoretical approach. In Sec. III, we describe details of the model and method of calculation. Our numerical results for the nonlinear susceptibility $\chi^{zzz}(-2\omega;\omega,\omega)$ are reported and discussed in Sec. IV. Finally we make conclusions in Sec. V.

II. THEORY

In this section we present a brief description of the formalism used to calculate the second-order nonlinear response, since this has already been reported with full details in Refs. [26,27]. The total susceptibility can be divided into two parts, $\chi^{abc}(-2\omega;\omega,\omega) = \chi_e^{abc}(-2\omega;\omega,\omega) + \chi_i^{abc}(-2\omega;\omega,\omega)$, where superscripts a, b, and c, denote Cartesian components. The imaginary part of the purely interband processes contribution is given by

$$\mathrm{Im}\left[\chi_e^{abc}\right] = \frac{\pi|e|^3}{\hbar^2}\int\frac{d^3k}{8\pi^3}\sum_{n\neq m\neq l}\left[\frac{2\mathrm{Re}\left[r^a_{nm}\left\{r^b_{ml}r^c_{ln}\right\}\right]}{\omega^S_{ml}-\omega^S_{ln}}\times\delta\left(\omega^S_{mn}-2\omega\right)+\left(\frac{\mathrm{Re}\left[r^a_{nl}\left\{r^b_{lm}r^c_{mn}\right\}\right]}{\omega^S_{mn}-\omega^S_{lm}}+\frac{\mathrm{Re}\left[r^a_{lm}\left\{r^b_{mn}r^c_{nl}\right\}\right]}{\omega^S_{nl}-\omega^S_{mn}}\right)\delta\left(\omega^S_{mn}-\omega\right)\right], \quad (1)$$

*alfonso@cio.mx

and the imaginary part of the mixed interband and intraband processes contribution is

$$\mathrm{Im}\left[\chi_i^{abc}\right] = \frac{\pi|e|^3}{\hbar^2}\int \frac{d^3k}{8\pi^3}\sum_{nm}\left[\left(\frac{2\mathrm{Im}\left[r^a_{nm}\left\{r^b_{mn;k^c}\right\}\right]}{\omega^S_{mn}} - \frac{4\mathrm{Im}\left[r^a_{nm}\left\{r^b_{mn}v^c_{mn}\right\}\right]}{(\omega^S)^2_{mn}}\right)\delta\left(\omega^S_{mn}-2\omega\right) + \left(\frac{\mathrm{Im}\left[\left\{r^a_{nm;k^c}r^b_{mn}\right\}\right]}{\omega^S_{mn}} + \frac{\mathrm{Im}\left[r^a_{nm}\left\{r^b_{mn}v^c_{mn}\right\}\right]}{(\omega^S)^2_{mn}} - \frac{\mathrm{Im}\left[\left\{r^b_{nm;k^a}r^c_{mn}\right\}\right]}{2\omega^S_{mn}}\right)\delta\left(\omega^S_{mn}-\omega\right)\right], \quad (2)$$

where r^a_{nm} are the matrix elements of the position operator between Bloch eigenstates $|\mathbf{k}n\rangle$ and $|\mathbf{k}m\rangle$ labeled by a band index n and crystal momentum $\mathbf{k}$. The electron charge is e and $\{\}$ implies the symmetrization of the Cartesian indices bc, i.e., $\{r^b_{mn}r^c_{nl}\} = (r^b_{mn}r^c_{nl} + r^c_{mn}r^b_{nl})/2$. The scissored energy difference is given by $\hbar\omega^S_{ml}(\mathbf{k}) = \hbar\omega^S_m(\mathbf{k}) - \hbar\omega^S_l(\mathbf{k})$, where $\hbar\omega^S_n(\mathbf{k}) = \hbar\omega_n(\mathbf{k}) + (1-f_n)\hbar\Delta$, $\hbar\omega_n$ being the energy of band n, f_n the Fermi occupation factor, and $\hbar\Delta$ the rigid energy GW gap correction at the Γ point. The generalized derivative of $\mathbf{r}$ is

$$r^a_{nm;k^c} = \frac{r^a_{nm}v^c_{mn} + r^c_{nm}v^a_{mn}}{\omega_{nm}} + \frac{i}{\omega_{nm}}\sum_l\left(\omega_{lm}r^c_{nl}r^v_{lm} - \omega_{nl}r^a_{nl}r^c_{lm}\right), \quad (n\neq m), \quad (3)$$

where $v^a_{nm} = (p^a_{nn} - p^a_{mm})/m_e$ is the difference between the electron velocities at bands n and m, and m_e is the electron mass.

We use a DFT-LDA calculation to obtain the energies and wave functions required by Eqs. (1) and (2). A more rigorous approach will use the many-body formalism using the GW approach [28,29]. The exact evaluation of the GW correction, for a full band structure along different symmetry lines in the Brillouin zone, can be an extremely demanding task. In the literature, it is quite standard to compute the GW corrections for several special $\mathbf{k}$ points and then to deduce a scissors correction. Thus a constant shift is applied to conduction-band DFT eigenvalues. The reliability of this GW scissors approximation has been recently discussed by Peelaers *et al.* [30] who compared the QP band structure and the DFT-LDA band structure with a scissors shift for Si and Ge nanowires. They found that the scissors approach is only valid for $\mathbf{k}$ points close to the Γ point and for bands close to the highest valence and lowest conduction bands. We can say with confidence that our results are reliable since the features observed in our calculated spectra come from transitions that take place between points close to the Γ point.

The GW approach yields very good results concerning the band structure. However having a good band structure is not enough if one is interested in linear and nonlinear optical response where one creates electron-hole excitations. Usually, in *ab initio* calculations of the linear response, the Bethe-Salpeter equation (BSE) is used to take into account the electron-hole interaction. However in the case of nonlinear response, much less is known about the impact of electron-hole correlation and exchange on the nonlinear response. Chang *et al.* [31] and Leitsman *et al.* [32] presented an *ab initio* many-body formalism for computing the SHG including excitonic effects. In their method, the electron-hole interaction was described through the Bether-Salpeter equation used for linear optics. The authors found a good agreement with experiment data in the static limit while in a large energy range the comparison with experimental is reasonable. Other formalisms have been developed but there is not a final theoretical approach [33–36]. This subject continues to be an open question and is both a theoretical challenge and a numerical challenge that ought to be pursued. This endeavor is beyond the scope of this paper.

III. COMPUTATIONAL METHOD

We have carried out *ab initio* pseudopotential DFT-LDA calculations to determine the equilibrium structures of pristine (5,0), (6,0), and (9,0) BNNTs. The theoretical equilibrium atomic positions and lattice constant were obtained when the forces acting on all the atoms were less than 0.003 eV/Å.

The calculation of the SHG response proceeds in three steps. We first determine the wave functions of the valence band states and a large number of conduction band states using DFT-LDA. In the second step, the quasiparticle correction to the DFT energy band gap E_{LDA} at the Γ point is evaluated within the GW approximation for the self-energy operator. Thus the band gap correction is given by $\Delta = (E_{\mathrm{GW}} - E_{\mathrm{LDA}})/\hbar$, E_{GW} being the GW energy band gap. The Brillouin zone integration is performed using a special $1\times1\times46$ wave-vector grid sampled within the Monkhorst-Pack scheme. The supercell method was used such that the NTs were aligned in a square array with a distance between adjacent nanotubes of at least 11 Å to prevent intertube interactions. We consider the NT oriented parallel to the z axis of the coordinate system. The screening potential W is treated by using the plasmon-pole model, a truncated Coulomb interaction with a cutoff of 10 Å in the radial direction, and also a cutoff of 80 Å in the tube axis direction. It is important to truncate the Coulomb interaction, otherwise the unphysical intertube interactions would increase the effective screening in the system and hence reduce the self-energy correction [37]. The self-energy Σ is obtained by summing over 24 vectors in the irreducible BZ, and over 250 bands. Finally in the third step, we evaluate the imaginary part of the SHG susceptibility by using Eqs. (1) and (2), which incorporate the corrections to the energy band gap through the scissors operator. Here, the Brillouin zone integration is performed using a special $2\times2\times600$ wave-vector grid sampled within the Monkhorst-Pack scheme. We obtain the real part of the second order susceptibility using the Kramers-Kronig relations [38].

All our *ab initio* calculations were performed by using the ABINIT package [39–41]. The wave functions were expanded onto a plane-wave basis set up to a kinetic energy cutoff of 30 Ha. The ion-electron interaction was approximated by Troullier-Martins pseudopotentials in the Kleinman-Bylander form.

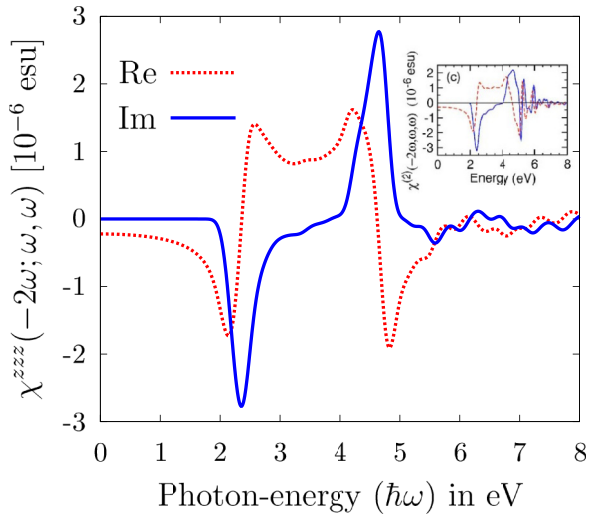

FIG. 1. (Color online) The calculated LDA ($\Delta = 0$) real and imaginary parts of $\chi^{zzz}(-2\omega;\omega,\omega)$ of a pristine zigzag (6,0) BNNT. In the inset we show Guo and Lin (Ref. [23]) LDA results for comparison.

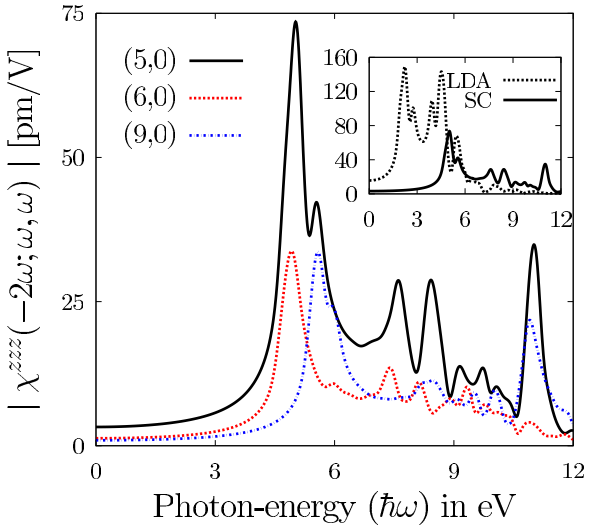

FIG. 2. (Color online) The calculated $|\chi^{zzz}(-2\omega;\omega,\omega)|$ for BN(5,0), BN(6,0), and BN(9,0) NTs including GW gap correction through the scissors operator. In the inset, we show $|\chi^{zzz}(-2\omega;\omega,\omega)|$ calculated with scissors (SC) and without scissors (LDA) correction for a BN(5,0) NT.

IV. RESULTS AND DISCUSSION

A. SHG of pristine BN nanotubes

We calculated the SHG susceptibility $\chi^{(2)}(-2\omega;\omega,\omega)$ of the pristine (5,0), (6,0), and (9,0) BNNTs. The point symmetry group of zigzag (n,0) NT is C_{2nv} [42]. Therefore, this symmetry group indicates that the following six components could be different from zero, namely $xxz = yyz = xzx$, $zyy = zxx$, and zzz. A very intense linear optical response is only observed for light polarized along the tube axis (z), since in the case of perpendicular polarization, the linear absorption is suppressed by strong depolarization effects [43]. Thus interband optical transition among valence and conduction bands around the Fermi level can be observable only for light polarized along the axial direction. Following this observation, we only consider the $\chi^{zzz}(-2\omega;\omega,\omega)$.

In Fig. 1, we display the LDA ($\Delta = 0$) real and imaginary parts of $\chi^{zzz}(-2\omega;\omega,\omega)$ for the (6,0) BNNT. Our results are in good qualitative agreement with those obtained by Guo and Lin presented in Fig. 2(c) of Ref. [23] and also included in the inset of our Fig. 1. Note that there is a good agreement between both results.

In Fig. 2, we show the absolute value of $\chi^{zzz}(-2\omega;\omega,\omega)$ calculated with the GW scissors correction for the (5,0), (6,0), and (9,0) BNNTs. In the three spectra we see a series of peaks which come from the first terms of Eqs. (1) and (2). All these features in the spectra are produced by two-photon transitions close to the Γ point at the center of the Brillouin zone. In the inset we show $|\chi^{zzz}|$ calculated with scissors and without scissors correction for the (5,0) BNNT. Note that the GW gap correction leads to a dramatic blueshift of the features as well as to a redistribution of the oscillator strength. $\chi^{zzz}(-2\omega;\omega,\omega)$ results of the three studied zigzag NTs yielded nonzero values whereas Guo and Lin reported that all components of $\chi(-2\omega;\omega,\omega)$ vanished numerically for (5,0) and (9,0) BNNTs including those components that could be different from zero according to the NT intrinsic symmetry.

The formulas we use for the calculation of the second order susceptibilities were obtained within the length gauge scheme and are such that the scissors operator is included. On the other hand, the formulas used by Guo and Lin were derived in Ref. [44] within the velocity gauge scheme, where the scissor operator was not introduced. Indeed, the correct way of introducing the effect of the scissors operator, within the velocity gauge, was done in Ref. [27], whereupon it was proved that both gauges satisfy gauge invariance, as they must, but only after the scissors operator is treated correctly. We remark that if the scissors correction is neglected, as done by Guo and Lin, then our formulas and the ones used by them are equivalent, again due to gauge invariance. Indeed, we have checked that both formulas give the same numerical results.

In Table I, we report the calculated LDA band gaps with scissors and without scissors GW correction, and also the static values of $\chi^{zzz}(0;0,0)$ for both cases. GW band gaps (scissored results) are bigger than DFT-LDA band gaps; meanwhile we note that the static value of $\chi^{zzz}(0;0,0)$ increases as the radius of the NT decreases. Also the static value is close to the theoretical static value of the zinc-blende (1.7 pm/V) bulk BN [45] and is smaller than that of the zinc-blende GaN whose theoretical value is 5.0 pm/V.

TABLE I. LDA and scissored (SC) band gaps of pristine BNNTs and their corresponding static values of $\chi^{zzz}(-2\omega;\omega,\omega)$.

	Band gap (eV)		$\chi^{zzz}(0;0,0)$ (pm/V)	
BNNT	LDA	SC	LDA	SC
(5,0)	2.0	7.6	15.7	3.3
(6,0)	2.6	7.7	7.3	1.3
(9,0)	3.6	9.9	6.0	0.9

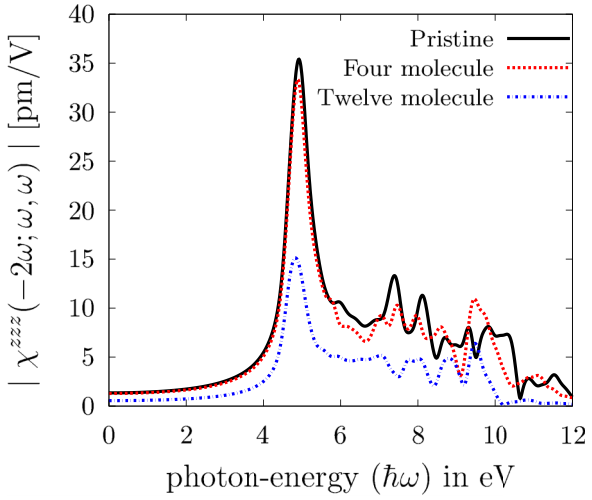

FIG. 3. (Color online) The calculated $|\chi^{zzz}(-2\omega;\omega,\omega)|$ for a zigzag (6,0) BNNT with increasing adsorbate coverage up to twelve hydrogen molecules per unit cell.

B. Molecular hydrogen adsorbed on BNNT outer surface

We now present results of the BNNT susceptibility $\chi^{zzz}(-2\omega;\omega,\omega)$ with hydrogen molecules adsorbed on the outer surface of the NT. For this study, we choose the zigzag (6,0) BNNT since it has been reported that the BNNTs are preferentially formed with zigzag orientation.

Our calculations show that the favorable adsorption sites are atop hexagon centers of NT surface. Hydrogen molecules are adsorbed in these sites forming an angle of 30° with respect to the axis of the nanotube. For a (6,0) BNNT, the NT surface has twelve hexagons per unit cell, therefore the maximum number of molecules that a (6,0) BNNT surface can absorb is twelve molecules per unit cell.

The calculated pristine (6,0) BNNT band gap including the GW gap correction is 7.7 eV which is in good agreement with the value of 7.6 eV obtained by Wirtz *et al.* [46] as a result of an *ab initio* calculation taking into account the GW correction. Recalling that hydrogen molecules exhibit weak interaction with the NT surface yielding physisorption, thus we expect a minimal perturbation on the structural and electronic properties. Therefore we shall expect a small variation in the band gap. In the case of twelve adsorbed molecules, we have obtained a band gap value of 7.7 eV.

Since the SHG signal is very sensitive to changes of the surface, here we test the usefulness for sensing the adsorption of molecules on the NT outer surface. In Fig. 3 we present $|\chi^{zzz}(-2\omega;\omega,\omega)|$ for a pristine NT and a NT with adsorption of four and twelve molecules per unit cell. Results indicate that the amplitude of the SHG signal decreases when the number of adsorbed hydrogen molecules increases. The static value of $\chi^{zzz}(0;0,0)$ shows the same behavior, it decreases from 1.30 (pm/V) for the pristine NT to 0.54 (pm/V) for the NT with twelve adsorbed molecules per unit cell.

V. CONCLUSIONS

We have presented SHG susceptibility *ab initio* calculations of single wall zigzag pristine BNNT and BNNTs modified by the molecular hydrogen adsorption on their outer surfaces. We have compared our results without scissors correction for the (6,0) BNNT with those reported by Guo and Lin [23] obtaining a very good agreement. However in the cases of the (5,0) and (9,0) BNNTs we found a nonvanishing SHG response, contrary to that found by Guo and Lin. We also found that the static value $\chi^{zzz}(0;0,0)$ increases as the NT radius decreases. Finally, calculations for BNNTs modified by molecular hydrogen adsorption demonstrate that an intensity decrease is obtained in the SHG spectrum as the number of hydrogen molecules increases. According to our results, SHG is a suitable technique to monitor the H_2 physisorption on the BNNT outer surface. We expect that our results may motivate the experimentalist community to investigate this class of NT surfaces.

ACKNOWLEDGMENT

We acknowledge support by CONACYT under Grant No. 153930.

[1] P. Singla, S. Singla, and N. Goel, Appl. Surf. Sci. **283**, 881 (2013).
[2] A. A. Peyghan, M. T. Baei, M. Moghimi, and S. Hashemian, J. Clust. Sci. **24**, 31 (2013).
[3] A. Soltani, S. G. Raz, V. J. Rezaei, A. D. Khalaji, and M. Savar, Appl. Surf. Sci. **263**, 619 (2012).
[4] J. Beheshtian, M. T. Baei, and A. Ahmadi, Surf. Sci. **606**, 981 (2012).
[5] D. Henwood and J. D. Carey, Phys. Rev. B **75**, 245413 (2007).
[6] S. Dag, Y. Ozturk, S. Ciraci, and T. Yildirim, Phys. Rev. B **72**, 155404 (2005).
[7] G. Chen, X. G. Gong, and C. T. Chan, Phys. Rev. B **72**, 045444 (2005).
[8] S. H. Jhi, Phys. Rev. B **74**, 155424 (2006).
[9] S. H. Jhi and Y. K. Kwon, Phys. Rev. B **69**, 245407 (2004).
[10] N. Arzate, R. A. Vázquez-Nava, and J. E. Mejía, Phys. Stat. Sol. C **5**, 2595 (2008).
[11] M. Breza, J. Mol. Struct. (Theochem) **767**, 159 (2006).
[12] X. M. Li, W. Q. Tian, X. R. Huang, C. C. Sun, and L. Jiang, J. Mol. Struct. (Theochem) **901**, 103 (2009).
[13] V. A. Margulis and E. E. Muryumin, Physica B **390**, 134 (2007).
[14] B. Xiao, J. Zhao, Y. Ding, and C. Sun, Surf. Sci. **604**, 1882 (2010).
[15] A. Ahmadi, M. Kamfiroozi, J. Beheshtian, and N. Hadipour, Struct. Chem. **22**, 1261 (2011).
[16] A. Ahmadi, J. Beheshtian, and N. Hadipour, Struct. Chem. **22**, 183 (2011).
[17] J. Dai, P. Giannozzi, and J. Yuan, Surf. Sci. **603**, 3234 (2009).
[18] F. C. Moraes, M. F. Cabral, L. H. Mascaro, and S. A. Machado, Surf. Sci. **605**, 435 (2011).
[19] S. S. Han, S. H. Lee, J. K. Kang, and H. M. Lee, Phys. Rev. B **72**, 113402 (2005).

[20] X. Wu, J. Yang, J. G. Hou, and Q. Zhu, Phys. Rev. B **69**, 153411 (2004).
[21] S. M. Dounce, M. Yang, and H. L. Dai, Surf. Sci. **565**, 27 (2004).
[22] U. Höfer, Appl. Phys. A **63**, 533 (1996).
[23] G. Y. Guo and J. C. Lin, Phys. Rev. B **72**, 075416 (2005).
[24] V. A. Margulis, E. E. Muryumin, and E. A. Gaiduk, Phys. Rev. B **82**, 235426 (2010).
[25] B. Adolph and F. Bechstedt, Phys. Rev. B **62**, 1706 (2000).
[26] F. Nastos, B. Olejnik, K. Schwarz, and J. E. Sipe, Phys. Rev. B **72**, 045223 (2005).
[27] J. L. Cabellos, B. S. Mendoza, M. A. Escobar, F. Nastos, and J. E. Sipe, Phys. Rev. B **80**, 155205 (2009).
[28] G. Onida, L. Reining, and A. Rubio, Rev. Mod. Phys. **74**, 601 (2002).
[29] L. Hedin, Phys. Rev. **139**, A796 (1965).
[30] H. Peelaers, B. Partoens, M. Giantomassi, T. Rangel, E. Goossens, G.-M. Rignanese, X. Gonze, and F. M. Peeters, Phys. Rev. B **83**, 045306 (2011).
[31] E. K. Chang, E. L. Shirley, and Z. H. Levine, Phys. Rev. B **65**, 035205 (2001).
[32] R. Leitsmann, W. G. Schmidt, P. H. Hahn, and F. Bechstedt, Phys. Rev. B **71**, 195209 (2005).
[33] E. Luppi, H. Hübener, and V. Véniard, J. Chem. Phys. **132**, 241104 (2010).
[34] E. Luppi, H. Hübener, and V. Véniard, Phys. Rev. B **82**, 235201 (2010).
[35] H. Hübener, E. Luppi, and V. Véniard, Phys. Rev. B **83**, 115205 (2011).
[36] M. L. Trolle, G. Seifert, and T. G. Pedersen, Phys. Rev. B **89**, 235410 (2014).
[37] C. D. Spataru, S. Ismail-Beigi, L. X. Benedict, and S. G. Louie, Appl. Phys. A **78**, 1129 (2004).
[38] N. Tancogne-Dejean, B. S. Mendoza, and V. Véniard, Phys. Rev. B **90**, 035212 (2014).
[39] The ABINIT code is a common project of the Université Catholique de Louvain, Corning Incorporated, and other contributors (URL http://www.abinit.org).
[40] X. Gonze, J.-M. Beuken, R. Caracas, F. Detraux, M. Fuchs, G.-M. Rignanese, L. Sindic, M. Verstraete, G. Zerah, F. Jollet, M. Torrent, A. Roy, M. Mikami, P. Ghosez, J.-Y. Raty, and D. Allan, Comput. Mater. Sci. **25**, 478 (2002).
[41] X. Gonze, G. M. Rignanese, M. Verstraete, J. Beuken, Y. Poillon, R. Caracas, F. Jollet, M. Torrent, G. Zerah, M. Mikami, P. Ghosez, M. Veithen, J. Y. Raty, V. Olevano, F. Bruneval, L. Reining, R. Godby, G. Onida, D. Hammann, and D. Allan, Zeit. für Kristallogr. **220**, 558 (2005).
[42] O. E. Alon, Phys. Rev. B **64**, 153408 (2001).
[43] H. Ajiki and T. Ando, Physica B **201**, 349 (1994).
[44] E. Ghahramani, D. J. Moss, and J. E. Sipe, Phys. Rev. B **43**, 8990 (1991).
[45] J. Chen, L. Jönsson, J. W. Wilkins, and Z. H. Levine, Phys. Rev. B **56**, 1787 (1997).
[46] L. Wirtz, A. Marini, and A. Rubio, Phys. Rev. Lett. **96**, 126104 (2006).